

Thermodynamics of the Polyakov-Nambu-Jona-Lasinio model with nonzero baryon and isospin chemical potentials

Swagato Mukherjee*

Department of Theoretical Physics, Tata Institute, of Fundamental Research, Homi Bhabha Road, Mumbai 400 005, India

Munshi G. Mustafa† and Rajarshi Ray‡

Theory Division, Saha Institute of Nuclear Physics, 1/AF, Bidhannagar, Kolkata 700 064, India

(Received 3 October 2006; published 16 May 2007)

We have extended the Polyakov-Nambu-Jona-Lasinio (PNJL) model for two degenerate flavors to include the isospin chemical potential (μ_I). All the diagonal and mixed derivatives of pressure with respect to the quark number (proportional to baryon number) chemical potential (μ_0) and isospin chemical potential up to sixth order have been extracted at $\mu_0 = \mu_I = 0$. These derivatives give the generalized susceptibilities with respect to quark and isospin numbers. Similar estimates for the flavor diagonal and off-diagonal susceptibilities are also presented. Comparison to lattice QCD (LQCD) data of some of these susceptibilities for which LQCD data are available show similar temperature dependence, though there are some quantitative deviations above the crossover temperature. We have also looked at the effects of instanton induced flavor mixing coming from the $U_A(1)$ chiral symmetry breaking 't Hooft determinantlike term in the NJL part of the model. The diagonal quark number and isospin susceptibilities are completely unaffected. The off-diagonal susceptibilities show significant dependence near the crossover. Finally we present the chemical potential dependence of specific heat and speed of sound within the limits of chemical potentials where neither diquarks nor pions can condense.

DOI: [10.1103/PhysRevD.75.094015](https://doi.org/10.1103/PhysRevD.75.094015)

PACS numbers: 12.38.Aw, 12.38.Mh, 12.39.-x

I. INTRODUCTION

Two of the most important features of strongly interacting matter at low temperature and chemical potentials are the phenomenon of color charge confinement and chiral symmetry breaking. However, with the increase in temperature and/or chemical potential, various phases may appear with different confining and chiral properties. At present both theoretical and experimental endeavors are underway to map out the phase diagram of QCD.

In the limit of infinite quark mass, the thermal average of the Polyakov loop can be considered as the order parameter for the confinement-deconfinement transition [1]. Though in the presence of dynamical quarks the Polyakov loop is not a rigorous order parameter for this transition, it still serves as an indicator of a rapid quark-hadron crossover. Motivated by this observation, Polyakov-loop based effective theories have been suggested [2–4] to capture the underlying physics of the confinement-deconfinement transition. The essential ingredient of these models is an effective potential constructed out of the Polyakov loop (and its complex conjugate). More recently, the parameters in these effective theories have been fixed [5,6] using the data from lattice QCD (LQCD) simulations (similar comparisons of perturbative effects on Polyakov loop with lattice data above the deconfinement transition was studied in [7]).

With the small quark masses the QCD Lagrangian has a partial global chiral symmetry, which is, however, broken spontaneously at low temperatures (and hence the absence of chiral partners of low-lying hadrons). This symmetry is supposed to be partially restored at higher temperatures and chemical potentials. The chiral condensate is considered to be the order parameter in this case. Various effective chiral models exist for the study of physics related to the chiral dynamics, e.g. the sigma model [8] and the Nambu-Jona-Lasinio (NJL) model [9,10]. The parameters of these models are fixed from the phenomenology of the hadronic sector.

Various studies of the QCD inspired models indicate (see e.g. Refs. [11–15]) that at low temperatures there is a possibility of first order phase transition for a large baryon chemical potential μ_B . This μ_{B_c} is supposed to decrease with increasing temperature. Thus, there is a first order phase transition line starting from $(T = 0, \mu_B = \mu_{B_c})$ on the μ_B axis in the (T, μ_B) phase diagram which steadily bends towards the $(T = T_c, \mu_B = 0)$ point and may actually terminate at a critical end point (CEP) characterized by $(T = T_E, \mu_B = \mu_{B_E})$, which can be detected via enhanced critical fluctuations in heavy-ion reactions [16]. The location of this CEP has become a topic of major importance in effective model studies (see e.g. Ref. [17]). For $\mu_B \neq 0$ LQCD has a complex determinant which hinders usual importance sampling techniques. However, recently the CEP was located for the physical [18] and for somewhat larger [19] quark masses using the reweighting technique of [20], and for the Taylor expansion method in [21].

*Electronic address: swagato@tifr.res.in†Electronic address: munshigolam.mustafa@saha.ac.in‡Electronic address: rajarshi.ray@saha.ac.in

For nonzero isospin chemical potential (μ_I) models and effective theories [22] find an interesting array of possible phases. The most important phenomenon that is supposed to happen is a transition to the pion condensed phase close to $\mu_I \sim m_\pi$. This has also been supported by lattice simulations [23], which does not suffer from the complex determinant problem for $\mu_I \neq 0$ and $\mu_B = 0$.

In this paper we study some of the thermodynamic properties of strongly interacting matter using the Polyakov-loop enhanced Nambu-Jona-Lasinio (PNJL) model [24,25]. In this model one is able to couple the chiral and deconfinement order parameters inside a single framework. While the NJL part is supposed to give the correct chiral properties, the Polyakov-loop part simulates the deconfinement physics. In fact studies of Polyakov loop coupled to chiral quark models have become quite fashionable these days (see e.g. Ref. [26]).

The initial motivation to couple Polyakov loop to the NJL model was to understand the coincidence of chiral symmetry restoration and deconfinement transitions observed in LQCD simulations [27]. While the NJL part is supposed to give the correct chiral properties, the Polyakov-loop part simulates the deconfinement physics. Indeed the PNJL model worked well to obtain the ‘‘coincidence’’ of onset of chiral restoration and deconfinement [24,25]. Recently the introduction of the Polyakov-loop potential [25,28] has made it possible to extract estimates of various thermodynamic quantities. The pressure, scaled pressure difference at various quark chemical potential μ_0 (or baryon chemical potential μ_B , where $\mu_B = 3\mu_0$), quark number density, and the interaction measure were extracted from the PNJL model in Ref. [28] for two quark flavors, and all the quantities compared well with the LQCD data. Following this, some of us made a comparative study [29] of the quark number susceptibility (QNS) and its higher order derivatives with respect to μ_0 with LQCD data. Here the qualitative features match very well though there are some quantitative differences. Very recently the spectral properties of low-lying meson states have been studied in [30].

Encouraged by these results, in this paper we have extended the the PNJL model to incorporate the effects of nonzero isospin chemical potential (μ_I). The motivation for this is that it enables one to calculate the isospin number susceptibility (INS) and its higher order derivatives with respect to μ_0 . LQCD data on these quantities are also available [31]. Thus comparing the results of PNJL for these quantities with that for the LQCD data will provide an opportunity to perform some stringent tests on the PNJL model.

Moreover, once both the QNS and the INS are known one can proceed further to compute the flavor-diagonal and off-diagonal susceptibilities separately. Since the second order flavor off-diagonal susceptibility measures the correlation among ‘‘up’’ (u) and ‘‘down’’ (d) flavors [32], this

quantity provide a direct understanding to the extent in which the PNJL model captures the underlying physics of QCD.

In our attempt to have a closer look at the u - d flavor correlation within the PNJL model, we have modified the NJL part of the PNJL model by using the NJL Lagrangian proposed in [33]. This Lagrangian has a term that can be interpreted as an interaction induced by instantons and reflects the $U_A(1)$ anomaly of QCD. It has the structure of a ’t Hooft determinant in the flavor space, leading to flavor mixing. By adjusting the relative strength of this term one can explicitly control the amount of flavor mixing in the NJL sector. This modified NJL Lagrangian reduces to the standard NJL Lagrangian [9,10] in some particular limit. This modification of the PNJL model has allowed us to study the effects of such flavor mixing on various susceptibilities, specially on the second order off-diagonal one which measures the u - d flavor correlation.

Investigation of the flavor-mixing effects brings us to an important issue regarding the NJL-type models. Within the framework of a NJL model it has been found [34] that for $\mu_I = 0$, in the $T - \mu_0$ plane, there is a single first order phase transition line (which ends at a critical end point) at low temperatures. But for $\mu_I \neq 0$ this single line separates into two first order phase transition lines because of the different behavior of the u and d quark condensates [35]. Thus there is a possibility of having two critical end points in the QCD phase diagram [35]. This has also been observed in random matrix models [36], in ladder QCD models [37], as well as in hadron resonance gas models [38]. It was then argued in Refs. [33,39] that the flavor mixing through the instanton effects [40,41] may wipe out this splitting. Later studies found that the splitting is considerable when μ_I is large [38,42] or μ_B is large [43]. We shall restrict ourselves only to small chemical potentials and calculate the susceptibilities with the modified PNJL model for different amounts of flavor mixing. Comparing these with LQCD data may give us some idea about the actual amount of the flavor mixing that is favored by the LQCD simulations.

Our next objective is to study the specific heat at constant volume (C_V) and speed of sound (v_s) of strongly interacting systems. These two quantities are of major importance for heavy-ion collision experiments. While C_V is related to the event-by-event temperature fluctuations [44] and mean transverse momentum fluctuations [45] in heavy-ion collisions, the quantity v_s controls the expansion rate of the fireball produced in such collisions and hence an important input parameter for the hydrodynamic studies [46–49]. The temperature dependence of these quantities was reported earlier in Ref. [29]. For the sake of completeness, in this paper we also have studied the quark number and isospin chemical potential dependence of C_V and v_s .

The plan of this paper is as follows. In Sec. II, we will present our formalisms. First, we will discuss briefly the extended PNJL model which we are going to use. Next, in

the same section, formalisms regarding the Taylor expansion of pressure (with respect to μ_0 and μ_I) and formulas for specific heat C_V and speed of sound v_s will be given. In Sec. III we will present our results and compare some of those with the available LQCD data. Finally, we conclude with a discussion in Sec. IV. Detail mathematical expressions regarding the model can be found in the appendix.

II. FORMALISM

A. PNJL model

The PNJL model at nonzero temperature T and quark number chemical potential μ_0 was introduced in

$$\Omega = \mathcal{U}(\Phi, \bar{\Phi}, T) + 2G_1(\sigma_u^2 + \sigma_d^2) + 4G_2\sigma_u\sigma_d - \sum_{f=u,d} 2T \int \frac{d^3p}{(2\pi)^3} \{ \ln[1 + 3(\Phi + \bar{\Phi}e^{-(E_f - \mu_f)/T})e^{-(E_f - \mu_f)/T} + e^{-3(E_f - \mu_f)/T}] + \ln[1 + 3(\bar{\Phi} + \Phi e^{-(E_f + \mu_f)/T})e^{-(E_f + \mu_f)/T} + e^{-3(E_f + \mu_f)/T}] \} - \sum_{f=u,d} 6 \int \frac{d^3p}{(2\pi)^3} E_f \theta(\Lambda^2 - \vec{p}^2). \quad (1)$$

Here for the two flavors the respective quark condensates are given by $\sigma_u = \langle \bar{u}u \rangle$ and $\sigma_d = \langle \bar{d}d \rangle$ ¹ and the respective chemical potentials are μ_u and μ_d . Note that $\mu_0 = (\mu_u + \mu_d)/2$ and $\mu_I = (\mu_u - \mu_d)/2$. The quasiparticle energies are $E_{u,d} = \sqrt{\vec{p}^2 + m_{u,d}^2}$, where $m_{u,d} = m_0 - 4G_1\sigma_{u,d} - 4G_2\sigma_{d,u}$ are the constituent quark masses and m_0 is the current quark mass (we assume flavor degeneracy). G_1 and G_2 are the effective coupling strengths of a local, chiral symmetric four-point interaction. Λ is the 3-momentum cutoff in the NJL model. $\mathcal{U}(\Phi, \bar{\Phi}, T)$ is the effective potential for the mean values of the traced Polyakov-loop Φ and its conjugate $\bar{\Phi}$, and T is the temperature. The functional form of the potential is

$$\frac{\mathcal{U}(\Phi, \bar{\Phi}, T)}{T^4} = -\frac{b_2(T)}{2} \bar{\Phi}\Phi - \frac{b_3}{6} (\Phi^3 + \bar{\Phi}^3) + \frac{b_4}{4} (\bar{\Phi}\Phi)^2, \quad (2)$$

with

$$b_2(T) = a_0 + a_1\left(\frac{T_0}{T}\right) + a_2\left(\frac{T_0}{T}\right)^2 + a_3\left(\frac{T_0}{T}\right)^3. \quad (3)$$

The coefficients a_i and b_i were fitted from LQCD data of pure gauge theory. The parameter T_0 is precisely the transition temperature for this theory, and as indicated by LQCD data its value was chosen to be 270 MeV [50–52]. With the coupling to the NJL model the transition does not remain first order. In this case from the peak in $d\Phi/dT$ the transition (or crossover) temperature T_c comes around 227 MeV.

Refs. [25,28]. Here we extend it to include the isospin chemical potential μ_I . We have introduced separate chemical potentials μ_u and μ_d for the up and down quark flavors, respectively, in the NJL model following Refs. [33,34]. To further extend it to include the Polyakov-loop dynamics we have followed the parameterization of the PNJL model used in Ref. [28]. We start with the final form of the mean-field thermodynamic potential per unit volume that we have obtained. It is given by (further details about the model can be found in the appendix)

Before we move further we note some important features of this model:

- (i) Since the gluons in this model are contained only in a static background field, the model would be suitable to study the physics below $T = 2.5T_c$. Above this temperature the transverse degrees of freedom become important [53].
- (ii) In general, pion condensation takes place in NJL models for $\mu_I > m_\pi/2$. Also there is a chiral transition for $\mu_0 \sim 340$ MeV above which diquark physics become important. For simplicity we neglect both the pion condensation and diquarks² and so restrict our analysis to $\mu_I < 70$ MeV and $\mu_0 < 200$ MeV.
- (iii) As discussed in the appendix, for $G_2 = 0$ the full symmetry of the Lagrangian in the chiral limit ($m_0 = 0$) is $SU_V(2) \times SU_A(2) \times U_V(1) \times U_A(1)$. The coefficient G_2 is interpreted as inducing instanton effects as it breaks the $U_A(1)$ symmetry explicitly by mixing the quark flavors. By using a parameterization $G_1 = (1 - \alpha)G_0$ and $G_2 = \alpha G_0$ (following Ref. [33]), one can tune the amount of instanton induced flavor mixing by varying α . For $\alpha = 0$ there is no instanton induced flavor mixing, and for $\alpha = 1$ the mixing becomes maximal. We shall look into the effects of this mixing in the susceptibilities.

The form of the NJL part in Eq. (1) is a generalization of the standard NJL model, which we get when $G_1 = G_2$, and $\mu_u = \mu_d$. In fact the potential in Eq. (1) becomes exactly the same as that of

¹Here we deviate from the convention of defining the sigma condensates from those of Refs. [28,29].

²Very recently diquarks have been discussed in Ref. [54] and pion condensation in Ref. [55].

Refs. [28,29] if we use $\alpha = 0.5$ and put G_0 equal to half the four-point coupling G in those references. We shall use this value for G_0 in this work.

- (iv) For the NJL sector without coupling to the Polyakov loop (i.e. setting $\Phi = \bar{\Phi} = 1$) one can easily see that the expression for Ω in Eq. (1), is invariant under the transformations $\mu_u \rightarrow -\mu_u$ “and/or” $\mu_d \rightarrow -\mu_d$. This implies that the physics along the directions of $\mu_0 = 0$ and $\mu_I = 0$ at any given temperature are equivalent. However, inclusion of the Polyakov loop turns off this symmetry. Now Ω is invariant only under the simultaneous transformation $\mu_u \rightarrow -\mu_u$ “and” $\mu_d \rightarrow -\mu_d$. This is a manifestation of the CP symmetry which implies that Ω is symmetric only under the simultaneous transformation $\Phi \rightarrow \bar{\Phi}$ and $\mu_{u,d} \rightarrow -\mu_{u,d}$ and vice versa. Thus coefficients of Φ and $\bar{\Phi}$ are found to be equal when $\mu_0 = 0$, and different when $\mu_I = 0$. In the $T - \mu_I$ plane we shall have $\Phi = \bar{\Phi}$, and everywhere else $\Phi \neq \bar{\Phi}$. This is reminiscent of the complex fermion determinant for nonzero μ_0 . This will be seen to have important consequences for the extraction of susceptibilities.
- (v) On the other hand, the quark condensates σ_u and σ_d are equal to each other whenever $\mu_0 = 0$ or $\mu_I = 0$ [see, e.g., Eq. (A18)] in the NJL as well as PNJL model. This can be seen by inspecting the thermodynamic potential Ω and remembering that we are using $G_1 + G_2 = G_0$, and also the fact that for $\mu_0 = 0$, $\Phi = \bar{\Phi}$. Now G_1 and G_2 are only coupled to the σ_u and σ_d . It is clear from Eq. (1) that whenever $\sigma_u = \sigma_d$, the couplings G_1 and G_2 come in the combination $G_1 + G_2 = G_0 = \text{constant}$. This means that the physics is completely independent of these couplings whenever either $\mu_0 = 0$ or $\mu_I = 0$.

B. Taylor expansion of pressure

The pressure as a function of temperature T , quark chemical potential μ_0 and isospin chemical potential μ_I is given by

$$P(T, \mu_0, \mu_I) = -\Omega(T, \mu_0, \mu_I). \quad (4)$$

Following usual thermodynamical relations, one can show that the first derivative of pressure with respect to μ_0 gives the quark number density. The second derivative is the quark number susceptibility. In LQCD since usual Monte Carlo importance sampling fails for nonzero μ_0 , the QNS and higher order derivatives computed at $\mu_0 = 0$ can be used as Taylor expansion coefficients to extract chemical potential dependence of pressure.

Given the thermodynamic potential Ω , our job is to minimize it with respect to the fields σ_u , σ_d , Φ , and $\bar{\Phi}$, using the following set of equations:

$$\frac{\partial \Omega}{\partial \sigma_u} = 0, \quad \frac{\partial \Omega}{\partial \sigma_d} = 0, \quad \frac{\partial \Omega}{\partial \Phi} = 0, \quad \frac{\partial \Omega}{\partial \bar{\Phi}} = 0. \quad (5)$$

The values of the fields so obtained can then be used to evaluate all the thermodynamic quantities in mean-field approximation. The crossover temperature for $\mu_0 = \mu_I = 0$ was obtained in Ref. [29] and was found to be $T_c = 227$ MeV. The field values obtained from Eq. (5) are then put back into Ω to obtain pressure from (4). We can then expand the scaled pressure at a given temperature in a Taylor series for the two chemical potentials μ_0 and μ_I ,

$$\frac{P(T, \mu_0, \mu_I)}{T^4} = \sum_{n=0}^{\infty} \sum_{j=0}^n \frac{n!}{j!(n-j)!} c_n^{jk}(T) \left(\frac{\mu_0}{T}\right)^j \left(\frac{\mu_I}{T}\right)^k; \quad k = n - j, \quad (6)$$

where,

$$c_n^{jk}(T) = \frac{1}{n!} \left. \frac{\partial^n (P(T, \mu_0, \mu_I)/T^4)}{\partial (\frac{\mu_0}{T})^j \partial (\frac{\mu_I}{T})^k} \right|_{\mu_0=0, \mu_I=0}. \quad (7)$$

The $n = \text{odd}$ terms vanish due to CP symmetry. Even for the $n = \text{even}$ terms, due to flavor degeneracy all the coefficients c_n^{jk} with j and k both odd vanish identically. In this work we evaluate all the 10 nonzero coefficients (including the pressure at $\mu_0 = \mu_I = 0$) up to order $n = 6$. Some of these coefficients have been measured already on the LQCD [31,56]. In our earlier work [29], we compared the 4 coefficients for $\mu_I = 0$ with those of the LQCD data using improved actions [31]. Here we shall be able to compare 3 more coefficients with LQCD data and also predict the behavior of the other 3 coefficients.

Let us now identify the coefficients which we shall compare with the LQCD data. The first set is given by

$$c_n^I(T) = \frac{1}{n!} \left. \frac{\partial^n (P(T, \mu_0)/T^4)}{\partial (\frac{\mu_0}{T})^n} \right|_{\mu_0=0} = c_n^{n0}. \quad (8)$$

These coefficients were already computed up to eighth order and compared to LQCD data to sixth order in [29]. The new set of coefficients to be compared with the LQCD data up to $n = 6$ are

$$c_n^I(T) = \frac{1}{n!} \left. \frac{\partial^n (P(T, \mu_0, \mu_I)/T^4)}{\partial (\frac{\mu_0}{T})^{n-2} \partial (\frac{\mu_I}{T})^2} \right|_{\mu_0=0, \mu_I=0} = c_n^{(n-2)2}; \quad n > 1. \quad (9)$$

The remaining coefficients we obtain are c_4^{04} , c_6^{24} , and c_6^{06} .

To complete the comparison with the LQCD data we have looked at the flavor-diagonal (c_n^{uu}) and flavor off-diagonal (c_n^{ud}) susceptibilities defined as

$$c_n^{uu} = \frac{c_n^{n0} + c_n^{(n-2)2}}{4}, \quad \text{and} \quad c_n^{ud} = \frac{c_n^{n0} - c_n^{(n-2)2}}{4}. \quad (10)$$

The second order flavor-diagonal and off-diagonal susceptibilities are given by

$$\begin{aligned} \frac{\chi_{uu}(T, \mu_u = 0, \mu_d = 0)}{T^2} &= \frac{\partial^2 P(T, \mu_u, \mu_d)}{\partial \mu_u^2} \Big|_{\mu_u = \mu_d = 0} \\ &= 2c_2^{uu}, \end{aligned}$$

and

$$\begin{aligned} \frac{\chi_{ud}(T, \mu_u = 0, \mu_d = 0)}{T^2} &= \frac{\partial^2 P(T, \mu_u, \mu_d)}{\partial \mu_u \partial \mu_d} \Big|_{\mu_u = \mu_d = 0} \\ &= 2c_2^{ud}. \end{aligned}$$

In this work we have computed all the coefficients using the following method. First the pressure is obtained as a function of μ_0 and μ_I for each value of T , and then fitted to a sixth order polynomial in μ_0 and μ_I . The quark number susceptibility, isospin number susceptibility, and all other higher order derivatives are then obtained from the coefficients of the polynomial extracted from the fit. In the fits we have used only the even order terms.

C. Specific heat and speed of sound

Given the thermodynamic potential Ω , the energy density ϵ is obtained from the relation,

$$\epsilon = -T^2 \frac{\partial(\Omega/T)}{\partial T} \Big|_V = -T \frac{\partial \Omega}{\partial T} \Big|_V + \Omega. \quad (11)$$

The rate of change of energy density ϵ with temperature at constant volume is the specific heat C_V which is given as,

$$C_V = \frac{\partial \epsilon}{\partial T} \Big|_V = -T \frac{\partial^2 \Omega}{\partial T^2} \Big|_V. \quad (12)$$

For a continuous phase transition one expects a divergence in C_V , which, as discussed earlier, will translate into highly enhanced transverse momentum fluctuations or highly suppressed temperature fluctuations if the dynamics in relativistic heavy-ion collisions is such that the system passes close to the CEP in the $T - \mu_B$ plane.

The square of velocity of sound at constant entropy S is given by

$$v_s^2 = \frac{\partial P}{\partial \epsilon} \Big|_S = \frac{\partial P}{\partial T} \Big|_V / \frac{\partial \epsilon}{\partial T} \Big|_V = \frac{\partial \Omega}{\partial T} \Big|_V / T \frac{\partial^2 \Omega}{\partial T^2} \Big|_V. \quad (13)$$

Since the denominator is nothing but the C_V , a divergence in specific heat would mean the velocity of sound going to zero at the CEP.

Given the relations Eq. (12) and (13), we first obtain the $\Omega(T, \mu_0 = 0)$ from the PNJL model. We then obtain the derivatives using the standard finite difference method. To get points close enough we have used cubic spline interpolations. This procedure has been repeated for various values of μ_0 and μ_I .

III. RESULTS

A. Taylor expansion of pressure

As discussed in Sec. II B, we extract the Taylor expansion coefficients by fitting the pressure as a function of μ_0 and μ_I at each temperature. Data for pressure was obtained in the range $0 < \mu_0 < 50$ MeV and $0 < \mu_I < 50$ MeV at all the temperatures. Spacing between consecutive data was kept at 0.1 MeV. We obtain all possible coefficients up to sixth order using the gnuplot³ program. The least-squares of all the fits came out to be 10^{-14} or less. This method was already used in our earlier work [29] where we checked the reliability of such fits. Here again we have reproduced all those coefficients satisfactorily. We shall first discuss the results with the standard flavor mixing in the NJL model parameterization (i.e. with $G_1 = G_2$) and then discuss the results for minimal ($G_2 = 0$) and maximal ($G_1 = 0$) flavor mixing.

I. $G_1 = G_2$

We start by presenting our results for the PNJL model with the standard NJL Lagrangian, i.e., $G_1 = G_2 = G_0/2$. Note that this is the case studied in the PNJL models of Refs. [25,28,29] but without the isospin chemical potential.

We present the QNS, INS and their higher order derivatives with respect to μ_0 in Fig. 1. We also have plotted the LQCD data from Ref. [31] for quantitative comparison. At the second order of Taylor expansion i.e. $n = 2$ we find (also observed earlier in [29]) that the QNS c_2 compares well with the LQCD data. On the other hand, the INS c_2^I quickly reaches its ideal gas value above T_c (around $2T_c$) in our model calculations, whereas the LQCD values are lower and match with the value of c_2 . Note that in the present form of the model the Polyakov loop itself rises a little above 1 and saturates. This leads to the INS to rise slightly above 1 at high temperatures. At the fourth order we see that the values of c_4 (also observed in [29]) in the PNJL model matches closely with those of LQCD data for up to $T \sim 1.05T_c$ and deviates significantly thereafter. The coefficient c_4^I is close to the LQCD data for the full range of T up to $2T_c$.

Earlier expectation [29,57] was that the mean-field analysis may not be sufficient and hence the higher order coefficient c_4 in the PNJL model shows significant departure from lattice results. This also should have meant that the INS c_2^I should be closer to LQCD data than c_4^I .

³See <http://www.gnuplot.info/>.

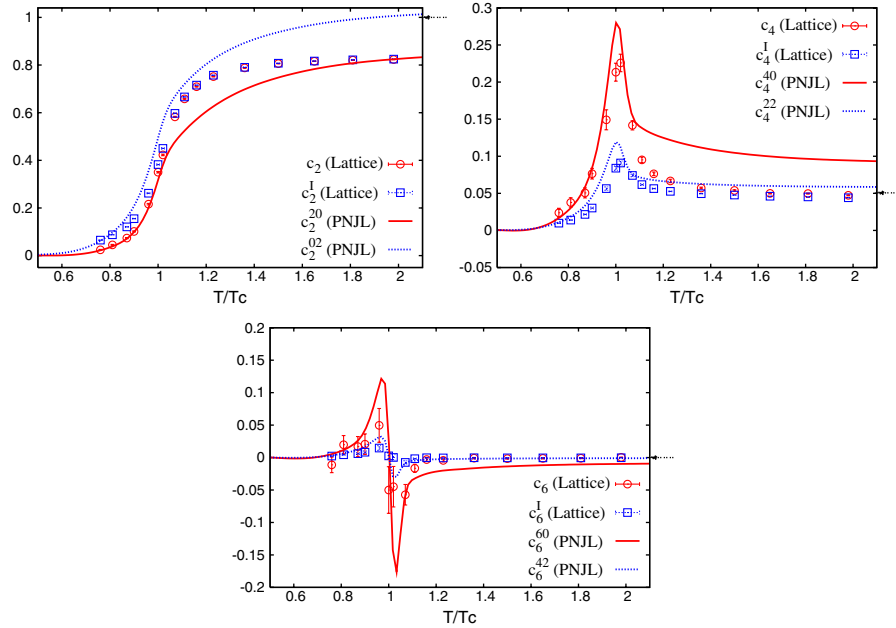


FIG. 1 (color online). The QNS and INS as functions of T/T_c . Symbols are LQCD data [31]. Arrows on the right indicate the corresponding ideal gas values.

However, our results show that the INS c_2^I is significantly different from the LQCD data above T_c , but c_4^I is quite consistent. Further, we see from Fig. 1 that both the sixth order coefficients c_6 and c_6^I are quite consistent with the LQCD results. We now give a qualitative explanation for the PNJL results and try to understand the behavior of the coefficients above T_c .

We pointed out in Sec. II A that in the thermodynamic potential Eq. (1), the Polyakov loop couples to μ_0 and its conjugate couples to $-\mu_0$ due to CP symmetry. As observed in the $SU(N)$ matrix model [58] and also in the PNJL model [28,29], this difference in coupling leads to splitting of the Polyakov loop and its conjugate for any nonzero μ_0 . Thus even at high temperatures when the Polyakov loop is close to 1, it decreases with increasing μ_0 and its conjugate increases (see left panel of Fig. 2). This means that the μ_0 dependence of pressure is not the same as that for an ideal gas. Hence the coefficients c_2 and

c_4 are both quite off from their respective ideal gas values. Also note that though c_6 is close enough, it is still distinctly different from zero. On the other hand for $\mu_0 = 0$, the Polyakov loop as well as its conjugate couples to both the μ_I and $-\mu_I$. They are, thus, equal (see right panel of Fig. 2) and also found to be almost constant for small μ_I . So the temperature dependence of the INS and its μ_I derivatives should reach the ideal gas behavior above T_c . For the coefficients which are mixed derivatives of μ_0 and μ_I , the behavior should be somewhere in between. And indeed we see that c_2^I , c_4^I , and c_6^I in Fig. 1 are quite close to their respective ideal gas values above T_c . Thus the LQCD results that show almost equal values of QNS and INS indicate that the splitting between the Polyakov loop and its conjugate in the $\mu_I = 0$ direction for $T > 1.5T_c$ is almost negligible (also supported by pQCD). This splitting was taken to be absolutely zero in the recent report with the PNJL model in Ref. [54].

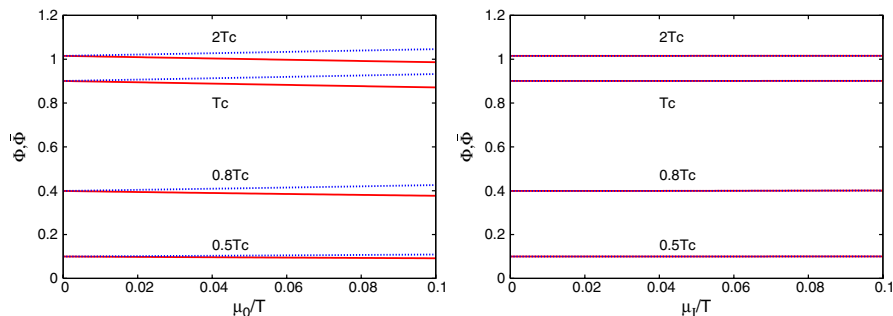


FIG. 2 (color online). Left panel: Φ (solid lines) decreases and $\bar{\Phi}$ (dotted lines) increases as a function of μ_0/T ($\mu_I = 0$). Right panel: Φ (solid lines) and $\bar{\Phi}$ (dotted lines) are equal and almost constant as a function of μ_I/T ($\mu_0 = 0$).

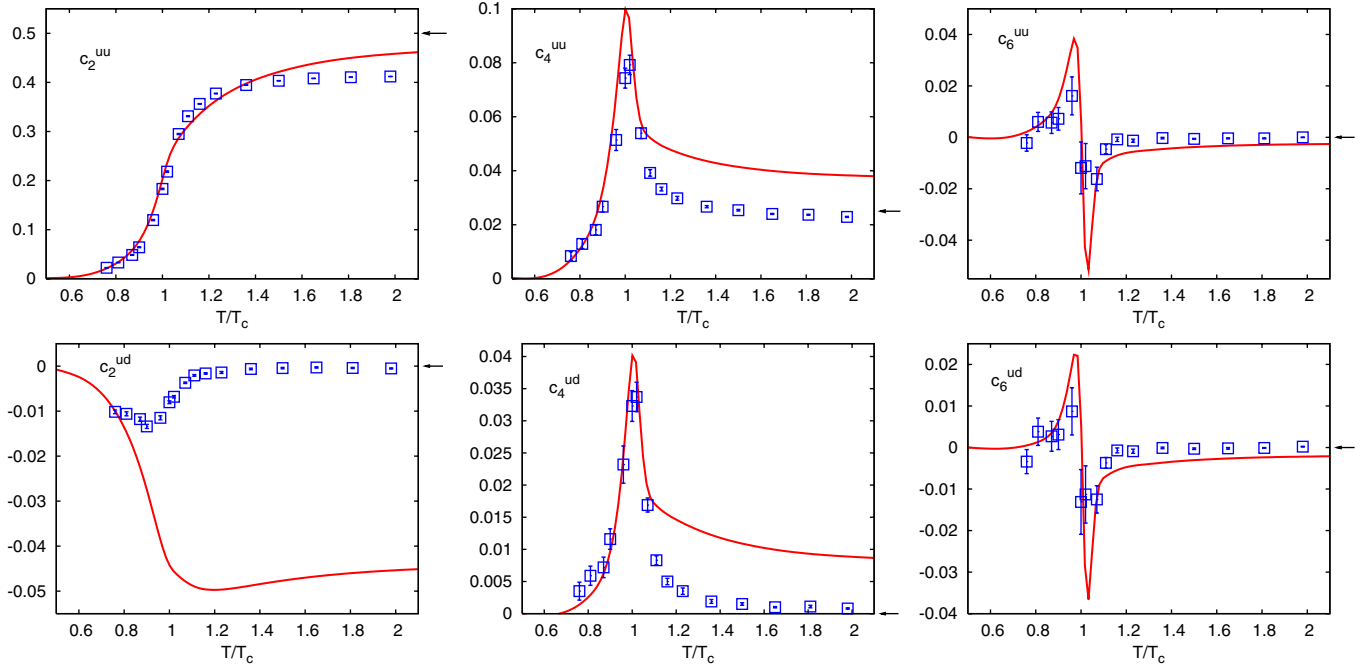


FIG. 3 (color online). The flavor diagonal (upper row) and flavor off-diagonal (lower row) susceptibilities for $n = 2, 4$, and 6 as functions of T/T_c . Symbols are LQCD data [31]. The arrows on the right indicate the respective ideal gas values.

In order to investigate these discrepancies between the results from the PNJL model and the LQCD data more closely, we have also calculated the flavor-diagonal (c_n^{uu}) and off-diagonal (c_n^{ud}) susceptibilities, defined in Sec. II B, up to sixth order. These are shown in Fig. 3. Except for c_2^{uu} , all the other LQCD results for flavor diagonal susceptibilities are close to their respective ideal gas values from around $1.2T_c$ onwards. The PNJL model values for the diagonal coefficient c_2^{uu} seem to be more or less consistent with the LQCD data. The most striking discrepancy with the LQCD data shows up in the second order flavor off-diagonal susceptibility c_2^{ud} . As discussed earlier, c_2^{ud} signifies the mixing of u and d quarks through the contribution of the two disconnected u and d quark loops. While the LQCD data shows that this kind of correlation between the u - d flavors are almost zero just away from T_c , the PNJL model results remains significant even up to $2T_c$. The

negativity of c_2^{ud} (see Fig. 3) indicates that the dominant correlation is between u quarks and d antiquarks and vice versa, i.e., pionlike. Hence putting in the dynamical pion condensate may throw some light on this issue. Also, addition of any new couplings (e.g. as shown for the isoscalar-vector and isovector-vector couplings for NJL model in Ref. [59]) may have important consequences for these susceptibilities.

Again from Fig. 3, the fourth order diagonal (c_4^{uu}) as well as the off-diagonal (c_4^{ud}) coefficients show a behavior similar to c_4^{uu} . Whereas the LQCD data reaches the ideal gas value above T_c , the PNJL values are quite distinctly separated. Finally, at the sixth order the behavior for both diagonal and off-diagonal coefficients in the PNJL model and LQCD are quite consistent.

We now present the temperature dependence of the remaining nonzero coefficients (Fig. 4). c_4^{04} is the fourth

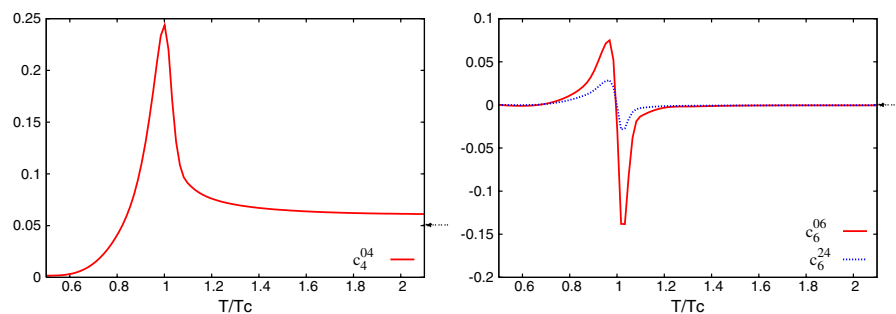


FIG. 4 (color online). c_4^{04} , c_6^{06} , and c_6^{24} as functions of T/T_c . Arrows on the right indicate the respective ideal gas values.

order diagonal coefficient in the isospin direction. In contrast to c_4^{40} we see that c_4^{04} approaches the ideal gas value quite fast above T_c . The behavior of c_6^{06} is quite similar to its counterpart c_6^{60} . This is in accordance to the expectation, as discussed earlier. The same is true for the coefficient c_6^{24} .

2. $G_1 \neq G_2$

Since the PNJL model has a problem in reproducing the LQCD data for c_2^{ud} which is a measure of the flavor-flavor correlation, it is interesting to have a closer look at the effect of flavor mixing on different susceptibilities. As discussed earlier, the parameterization $G_1 = (1 - \alpha)G_0$ and $G_2 = \alpha G_0$ enables one to tune the instanton induced flavor mixing by varying the value of α between 0 and 1. Here we discuss the two extreme cases of $\alpha = 1$ (maximal mixing) and $\alpha = 0$ (zero mixing). We have recalculated all c_n and c_n^I , up to $n = 6$, for $\alpha = 0$, and, 1. We found that all the diagonal coefficients, including c_2^I and c_4 whose behavior are the most drastically different in the PNJL model and in LQCD, are independent of the values of α . As a consequence, the second order flavor off-diagonal susceptibility [$c_2^{ud} = (c_2^I - c_2)/4$] is also unaffected by the instanton induced flavor-mixing effects.

The above fact can be understood from the following reasoning. We mentioned in Sec. II A that the quark condensates σ_u and σ_d are equal to each other for either of the cases $\mu_0 = 0$ and $\mu_I = 0$. This is clear from Eq. (A18). Now G_1 and G_2 couple only to the σ_u and σ_d . So for $\sigma_u = \sigma_d$, we only get the combination $G_1 + G_2 = G_0$, which is a constant. Thus none of the physics in the $\mu_0 = 0$ and $\mu_I = 0$ directions depend on the value of α , implying that the diagonal derivatives in these two directions will also be independent of α .

However, the mixed derivatives can have dependence on α . This is because the values of σ_u and σ_d can be different when both μ_0 and μ_I are together nonzero. This was seen in Ref. [33] for the normal NJL model. But those authors also found that there is a critical value of $\alpha_c \approx 0.11$ above which the condensates σ_u and σ_d become equal even for both μ_0 and μ_I being nonzero. Here, for the PNJL model we have found that all the mixed derivatives up to sixth

order are exactly equal for the two cases $\alpha = 0.5$ (standard mixing used in NJL and PNJL models) and $\alpha = 1$ (maximal mixing) which is in accordance to the results of the above reference. We hope to obtain the value for α_c for the PNJL model in the future. For $\alpha = 0$, all the off-diagonal coefficients were found to differ from those at $\alpha = 0.5$.

The left-most panel in Fig. 5 shows the independence of c_2^{ud} on α . The rest of the figures show one representative coefficient each for $n = 4$, and 6. As can be seen, the instanton effects quite significantly suppress the temperature variation of these coefficients near T_c . Also it can be observed from Fig. 5, that the LQCD data favors a larger amount of instanton induced flavor mixing.

B. Dependence of C_V and v_s^2 on μ_0 and μ_I

Here we present the chemical potential dependence of specific heat C_V and the speed of sound v_s . The range of the three representative values of μ_0 and μ_I are such that neither the diquark physics nor the pion condensation becomes important. In the ideal gas limit the expression for C_V is as a function of temperature T and either of the chemical potentials μ_0 or μ_I is given by $C_V/T^3 = (74\pi^2/15) + 6(\mu_{0,I}^2/T^2)$. Thus, for large temperatures and not so large chemical potentials, it can be expected that the C_V is more or less independent of $\mu_{0,I}$'s. This is borne out in the PNJL model as seen in Fig. 6. At low temperatures, however, there can be a nontrivial contribution from chemical potential. As illustrated in Fig. 6, the low temperature behavior is away from ideal gas, but there is a significant difference in the values of C_V as a function of μ_0 . In the range of μ_I considered, even for $T < T_c$ there seems to be no significant isospin effects. Another interesting feature is that as a function of μ_0 , the peak of C_V which appears at T_c shifts towards lower temperatures. This signifies that the transition temperature may decrease and also the nature of transition may change as the chemical potentials increase. A decrease of T_c with increasing μ_0 and μ_I is consistent with what has been found on the lattice [60,61]. We hope to address this issue through the analysis of chiral susceptibility in a future publication.

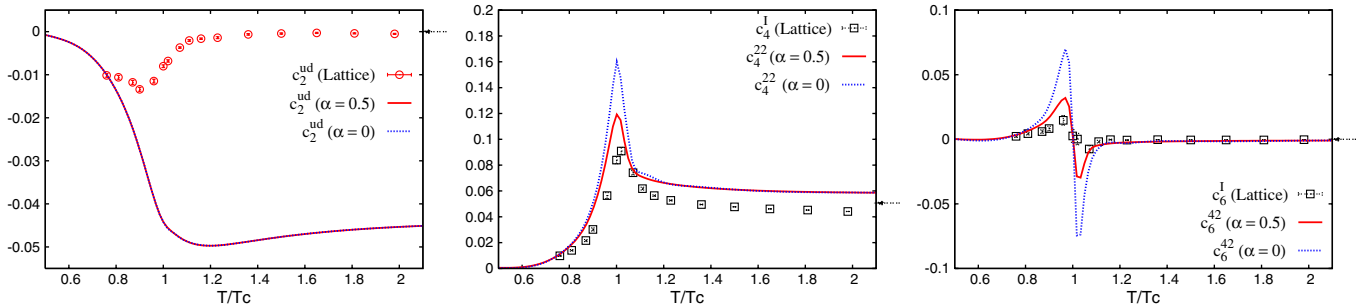


FIG. 5 (color online). Left panel: c_2^{ud} is independent of α . Middle and right panels: dependence of some off-diagonal coefficients on the flavor-mixing parameter α . Symbols are lattice data [31]. Arrows on the right indicate the corresponding ideal gas values.

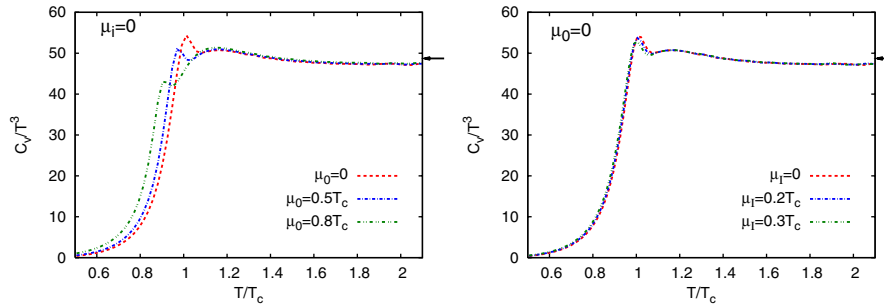


FIG. 6 (color online). C_V as a function of T/T_c . Left panel shows the variation with μ_0 . Right panel shows the variation with μ_I . Arrows on the right indicate the ideal gas value for $\mu_0 = \mu_I = 0$.

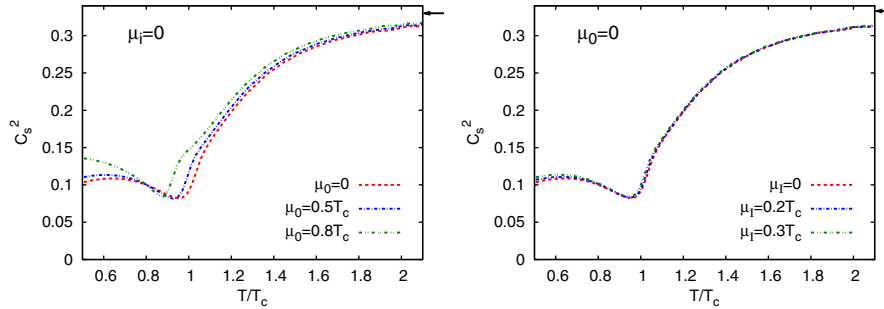


FIG. 7 (color online). v_s^2 as a function of T/T_c . Left panel shows the variation with μ_0 . Right panel shows the variation with μ_I . Arrows on the right indicate the ideal gas value for $\mu_0 = \mu_I = 0$.

The speed of sound in the ideal gas limit is the same $\sqrt{3}$ for any given temperature and chemical potential. As shown in Fig. 7 the v_s^2 for different μ_0 and μ_I merges towards the ideal gas value at large temperatures. However, even above T_c , there is significant increase in v_s^2 for increase in μ_0 . So for nonzero quark matter density the speed of sound is higher near T_c and this may have important contribution to thermalization of the matter created in relativistic heavy-ion collision experiments. Again there seems to be negligible isospin dependence of c_s^2 in the range of temperatures studied. From Fig. 7 we note that in the PNJL model even with μ_0 as large as $0.8T_c$, the v_s^2 never reaches a value as large as 0.2 near or below $T = T_c$ which was used in [62] to describe the rapidity spectra.

IV. DISCUSSIONS AND SUMMARY

We have extended the PNJL model of Ref. [28] by the introduction of isospin chemical potential. Using this we have studied the behavior of strongly interacting matter with two degenerate quark flavors in the phase space of T , μ_0 , and μ_I , for small values of the chemical potentials. We have extracted 10 coefficients of Taylor expansion of pressure in the two chemical potentials up to sixth order. Some of these coefficients were compared with available LQCD data. The quark number susceptibility and isospin susceptibility show order parameterlike behavior. A quantitative

comparison shows that the quark number susceptibility reaches about 85% of its ideal gas value up to temperature of about $2T_c$, consistent with LQCD results. However, the isospin susceptibility reaches its ideal gas value by this temperature. This is in contrast to LQCD results where both the susceptibilities are almost equal from around $1.2T_c$ onward. Similarly, the higher order derivatives for μ_I approach the ideal gas behavior much faster compared to those for μ_0 . In contrast, though both the QNS and INS in LQCD deviate from their ideal gas values, the higher order derivatives reach their ideal gas limit quickly. The values of the mixed derivatives in the PNJL model shows a behavior somewhat in between. On the lattice however, the mixed derivatives are almost zero (i.e., the ideal gas value) above T_c .

Thus some of the coefficients in the PNJL model differ from the LQCD data and one could hold the mean-field analysis responsible for this departure. But if this argument were true then the higher order derivatives obtained in the PNJL model should depart from the LQCD data more than the lower order coefficients, which is not the case. Against this expectation, we have found a very nice pattern in the PNJL results which can be understood in terms of the behavior of the Polyakov loop. The dependence of the Polyakov loop and its conjugate on temperature and the chemical potentials is extremely important. For $\mu_I = 0$ they have different values when μ_0 is varied. This makes

all the coefficients which are derivatives of pressure with respect to μ_0 alone, to deviate from the ideal gas behavior. For $\mu_0 = 0$, however, the Polyakov loop and its conjugate are equal and hence both reach the ideal gas value above T_c . Thus the coefficients which are derivatives of pressure with respect to μ_l alone, all reach their respective ideal gas values above T_c . The mixed derivatives are found to be somewhere in between. Nonetheless, we hope to look into the effects of fluctuations in the future.

In order to have a closer look at the discrepancy between the PNJL results and LQCD data, we have also calculated the flavor-diagonal and flavor off-diagonal susceptibilities up to sixth order. We have found that the second order flavor off-diagonal susceptibility, which indicates the correlation among up and down quarks, is significantly away from zero even up to $T = 2T_c$. On the other hand, LQCD results [63] show that correlation among the flavors in the second order off-diagonal susceptibility is largely governed by the interaction of the quarks with the gauge fields and is almost independent of the presence of the quarks loops. This motivated us to study the instanton induced flavor-mixing effects within the framework of the PNJL model. Unfortunately, we found no effect of flavor mixing on any diagonal QNS and INS, and hence on the second order flavor off-diagonal susceptibility. We speculate one possibility to reconcile PNJL and LQCD data, that is to keep the pion condensate as a dynamical variable and perform the calculations. In fact there are indications [64] that at zero temperature and in the chiral limit, pion condensation can be catalyzed by an external chromomagnetic field. We hope to present these results in the future.

On the other hand, flavor-mixing effects on the mixed susceptibilities of quark and isospin chemical potentials indicate that large flavor mixing is favored by the LQCD data. This may have important consequences [33] on the phase diagram of the NJL model at low temperature and large baryon chemical potential.

Apart from the possible improvements for the Polyakov-loop potential, inclusion of pionic and diquark fluctuations, etc. we also intend to include terms in the NJL part with six point couplings to take proper account of the quark number fluctuations in the low temperature phase.

We also have investigated chemical potential dependence of specific heat and speed of sound. The specific heat sort of becomes independent of chemical potential just above T_c . Below T_c there is some significant effect from both the chemical potentials μ_0 and μ_l . Consistent with LQCD findings [60,61], the peak in specific heat towards lower temperatures with increasing chemical potentials indicates a decrease in the transition temperature. We plan to make a more detailed investigation of the location of the phase boundary. The speed of sound, on the other hand, increases with the increase of either of the chemical potentials in almost the whole range of temperatures. But this dependence becomes milder as one goes to higher

temperatures. Thus with a proper implementation of the PNJL equation of state into the hydrodynamic studies of elliptic flow, one may be able to make some estimates of both the temperature and densities reached in the heavy-ion collision experiments.

ACKNOWLEDGMENTS

R.R. would like to thank S. Dital for many useful discussions and comments.

APPENDIX

Here we present the complete details of the PNJL model used in our work. First we discuss the NJL model in the complete space of temperature T and the up and down flavor chemical potentials μ_u and μ_d (or equivalently the quark chemical potential μ_0 and isospin chemical potential μ_l) [33,34]. Then we extend it to couple with the Polyakov loop.

1. The NJL model

The NJL model Lagrangian for two flavors can be written as [33,34]

$$\mathcal{L} = \mathcal{L}_0 + \mathcal{L}_1 + \mathcal{L}_2, \quad (\text{A1a})$$

$$\mathcal{L}_0 = \bar{\psi}(i\partial/ - m)\psi, \quad (\text{A1b})$$

$$\mathcal{L}_1 = G_1[(\bar{\psi}\psi)^2 + (\bar{\psi}\vec{\tau}\psi)^2 + (\bar{\psi}i\gamma_5\psi)^2 + (\bar{\psi}i\gamma_5\vec{\tau}\psi)^2], \quad (\text{A1c})$$

$$\mathcal{L}_2 = G_2[(\bar{\psi}\psi)^2 - (\bar{\psi}\vec{\tau}\psi)^2 - (\bar{\psi}i\gamma_5\psi)^2 + (\bar{\psi}i\gamma_5\vec{\tau}\psi)^2], \quad (\text{A1d})$$

where

$$\psi = (u, d)^T, \quad [G_1] = [G_2] = [\text{energy}]^{-2}, \quad (\text{A2})$$

$$m = \text{diag}(m_u, m_d).$$

We shall assume flavor degeneracy $m_u = m_d = m_0$. For $m_0 = 0$ the symmetries of the different parts of the Lagrangian (A1) are

$$\mathcal{L}_0: SU_V(2) \times SU_A(2) \times U_V(1) \times U_A(1), \quad (\text{A3a})$$

$$\mathcal{L}_1: SU_V(2) \times SU_A(2) \times U_V(1) \times U_A(1), \quad (\text{A3b})$$

$$\mathcal{L}_2: SU_V(2) \times SU_A(2) \times U_V(1). \quad (\text{A3c})$$

\mathcal{L}_2 has the structure of a 't Hooft determinant, $\det[\bar{q}(1 + \gamma_5)q] + \det[\bar{q}(1 - \gamma_5)q]$ [10] and breaks $U_A(1)$ axial symmetry. This interaction can be interpreted as being induced by instantons and reflects the $U_A(1)$ anomaly of QCD.

We are interested in the properties of this Lagrangian at nonzero temperatures T and chemical potentials μ_u and μ_d . Equivalently, one also can use the quark number chemical potential $\mu_0 = (\mu_u + \mu_d)/2$ and the isospin

chemical potential $\mu_I = (\mu_u - \mu_d)/2$. In the mean-field approximation we consider the two quark condensates $\sigma_u = \langle \bar{u}u \rangle$ and $\sigma_d = \langle \bar{d}d \rangle$. The pion condensate $\vec{\pi}$ is assumed to be zero (which is true in the NJL model for $\mu_I < m_\pi/2$). Then the thermodynamic potential is obtained as

$$\Omega(T, \mu_u, \mu_d) = \sum_{f=u,d} \Omega_0(T, \mu_f; m_f) + 2G_1(\sigma_u^2 + \sigma_d^2) + 4G_2\sigma_u\sigma_d, \quad (\text{A4a})$$

$$\begin{aligned} \Omega_0(T, \mu_f; m_f) = & -2N_c \int \frac{d^3p}{(2\pi)^3} E_f \theta(\Lambda^2 - \vec{p}^2) \\ & - 2N_c T \int \frac{d^3p}{(2\pi)^3} \ln[1 + e^{-(E_f - \mu_f)/T}] \\ & - 2N_c T \int \frac{d^3p}{(2\pi)^3} \ln[1 + e^{-(E_f + \mu_f)/T}], \end{aligned} \quad (\text{A4b})$$

where the energy E_f and constituent quark mass m_f is given by

$$E_f = \sqrt{m_f^2 + p^2}, \quad (\text{A5})$$

$$m_f = m_0 - 4G_1\sigma_f - 4G_2\sigma_{f'}, \quad f \neq f' \in \{u, d\}. \quad (\text{A6})$$

Finding the stationary points of the thermodynamic potential with respect to σ_u and σ_d , i.e., solving the coupled equations $\partial\Omega/\partial\sigma_u = 0$ and $\partial\Omega/\partial\sigma_d = 0$, one gets the gap equations

$$\sigma_f = -2N_c \int \frac{d^3p}{(2\pi)^3} \frac{m_f}{E_f} [\theta(\Lambda^2 - p^2) - n(E_f) - \bar{n}(E_f)], \quad f = u, d, \quad (\text{A7a})$$

$$n(E_f) = \frac{1}{1 + \exp(E_f - \mu_f)}, \quad \text{and}$$

$$\bar{n}(E_f) = \frac{1}{1 + \exp(E_f + \mu_f)}. \quad (\text{A7})$$

The constituent mass m_f for one flavor depends in general on both the condensates [see Eq. (A6)] and therefore the two flavors are coupled. Chiral symmetry [$SU_A(2)$] is broken spontaneously for $\sigma_f \neq 0$. Let us now make the parameterization

$$G_1 = (1 - \alpha)G_0, \quad \text{and} \quad G_2 = \alpha G_0 \quad (\text{A8})$$

with a fixed value of G_0 . Tuning the value of α one can control the flavor mixing in the Lagrangian. We consider some of the cases below.

- (1) $\alpha = 0$: This implies $G_2 = 0$ i.e. the $U_A(1)$ symmetry breaking term \mathcal{L}_2 drops out and hence \mathcal{L} has no flavor mixing.

- (2) $\alpha = 1$: Here $G_1 = 0$, and thus \mathcal{L}_2 completely dominates the coupling. The flavor mixing in \mathcal{L} is thus “maximal.”

- (3) $\alpha = 1/2$: In this case we have $G_1 = G_2 = G_0/2$. So the Lagrangian $\mathcal{L} = \mathcal{L}_0 + G_0[(\bar{\psi}\psi)^2 + (\bar{\psi}i\gamma_5\vec{\tau}\psi)^2]$, is the standard NJL model [9]. Here also the $U_A(1)$ symmetry is broken which is commensurate with the fact that in nature the η particle is much heavier than the π 's.

2. Extension to PNJL

Our aim is to extend the PNJL model introduced in Refs. [25,28] to include isospin chemical potential. To achieve this we now include the Polyakov loop and its effective potential to the NJL model described above. The Lagrangian becomes

$$\mathcal{L}_{\text{PNJL}} = \mathcal{L}_0 + \mathcal{L}_1 + \mathcal{L}_2 - \mathcal{U}(\Phi[A], \bar{\Phi}[A], T). \quad (\text{A9})$$

The only part of the NJL sector that is modified is \mathcal{L}_0 which now becomes

$$\mathcal{L}_0 = \bar{\psi}(iD/ - m)\psi, \quad (\text{A10})$$

where

$$\begin{aligned} D^\mu = \partial^\mu - iA^\mu, \quad A^\mu = \delta_{\mu 0}A^0, \\ A^\mu(x) = g\mathcal{A}_a^\mu(x)\lambda_a/2. \end{aligned} \quad (\text{A11})$$

$\mathcal{A}_a^\mu(x)$ are $SU(3)$ gauge fields and λ_a are Gell-Mann matrices.

$\mathcal{U}(\Phi[A], \bar{\Phi}[A], T)$ is the effective potential expressed in terms of the traced (over color) Polyakov loop (with periodic boundary conditions) and its charge conjugate:

$$\begin{aligned} \Phi = \frac{\text{Tr}_c L}{N_c}, \quad \bar{\Phi} = \frac{\text{Tr}_c L^\dagger}{N_c}, \\ L(\vec{x}) = \mathcal{P} \exp \left[i \int_0^\beta d\tau A_4(\vec{x}, \tau) \right], \quad \beta = \frac{1}{T}, \\ A_4 = iA_0. \end{aligned} \quad (\text{A12})$$

We shall be working in the mean-field limit. For simplicity of notation we shall use Φ and $\bar{\Phi}$ as their respective mean fields. Φ is the order parameter for deconfinement transition. In the absence of quarks $\Phi = \bar{\Phi}$ and deconfinement is associated with the spontaneous breaking of the $Z(3)$ symmetry. Conforming to this symmetry and parameterizing the LQCD Monte Carlo data one can write down an effective potential for Φ and $\bar{\Phi}$. Following Ref. [28], we write

$$\frac{\mathcal{U}(\Phi, \bar{\Phi}, T)}{T^4} = -\frac{b_2(T)}{2}\Phi\bar{\Phi} - \frac{b_3}{6}(\Phi^3 + \bar{\Phi}^3) + \frac{b_4}{4}(\bar{\Phi}\Phi)^2, \quad (\text{A13a})$$

$$b_2(T) = a_0 + a_1\left(\frac{T_0}{T}\right) + a_2\left(\frac{T_0}{T}\right)^2 + a_3\left(\frac{T_0}{T}\right)^3. \quad (\text{A13b})$$

At low temperature \mathcal{U} has a single minimum at $\Phi = 0$,

while at high temperatures it develops a second one which turns into the absolute minimum above a critical temperature T_0 . Φ and $\bar{\Phi}$ will be treated as independent classical fields. The mean-field analysis of the NJL part of the model proceeds in exactly the same way as in the previous case. Using σ_u and σ_d as the independent quark condensates (and neglecting $\vec{\pi}$) one gets the expression for the thermodynamic potential,

$$\Omega(T, \mu_u, \mu_d) = \mathcal{U}(\Phi, \bar{\Phi}, T) + \sum_{f=u,d} \Omega_0(T, \mu_f; M_f) + 2G_1(\sigma_u^2 + \sigma_d^2) + 4G_2\sigma_u\sigma_d, \quad (\text{A14a})$$

$$\begin{aligned} \Omega_0(T, \mu_f; M_f) = & -2N_c \int \frac{d^3p}{(2\pi)^3} E_f \theta(\Lambda^2 - \vec{p}^2) - 2T \int \frac{d^3p}{(2\pi)^3} \text{Tr}_c \ln[1 + L e^{-(E_f - \mu_f)/T}] \\ & - 2T \int \frac{d^3p}{(2\pi)^3} \text{Tr}_c \ln[1 + L^\dagger e^{-(E_f + \mu_f)/T}], \end{aligned} \quad (\text{A14b})$$

where $E_{u,d} = \sqrt{m_{u,d}^2 + p^2}$ and $m_{u,d} = m_0 - 4G_1\sigma_{u,d} - 4G_2\sigma_{d,u}$.

Note that with $\alpha = 0.5$ and $\mu_u = \mu_d = \mu$ and if for the coupling G and condensate σ of Ref. [28] one uses $G = 2G_0$ and $\sigma = \sigma_u + \sigma_d$, then the thermodynamic potentials here and in Ref. [28] are exactly equal.

Using the identity $\text{Tr} \ln X = \text{Indet} X$ one can write for a given flavor f ,

$$\begin{aligned} \text{Indet}[1 + L e^{-(E_f - \mu_f)/T}] + \text{Indet}[1 + L^\dagger e^{-(E_f + \mu_f)/T}] = & \ln[1 + 3(\Phi + \bar{\Phi} e^{-(E_f - \mu_f)/T}) e^{-(E_f - \mu_f)/T} + e^{-3(E_f - \mu_f)/T}] \\ & + \ln[1 + 3(\bar{\Phi} + \Phi e^{-(E_f + \mu_f)/T}) e^{-(E_f + \mu_f)/T} + e^{-3(E_f + \mu_f)/T}]. \end{aligned} \quad (\text{A15})$$

This gives us the final form of the thermodynamic potential as

$$\Omega(T, \mu_u, \mu_d) = \mathcal{U}(\Phi, \bar{\Phi}, T) + \sum_{f=u,d} \Omega_0(T, \mu_f; M_f) + 2G_1(\sigma_u^2 + \sigma_d^2) + 4G_2\sigma_u\sigma_d, \quad (\text{A16a})$$

$$\begin{aligned} \Omega_0(T, \mu_f; M_f) = & -2N_c \int \frac{d^3p}{(2\pi)^3} E_f \theta(\Lambda^2 - \vec{p}^2) - 2T \int \frac{d^3p}{(2\pi)^3} \ln[1 + 3(\Phi + \bar{\Phi} e^{-(E_f - \mu_f)/T}) e^{-(E_f - \mu_f)/T} \\ & + e^{-3(E_f - \mu_f)/T}] - 2T \int \frac{d^3p}{(2\pi)^3} \ln[1 + 3(\bar{\Phi} + \Phi e^{-(E_f + \mu_f)/T}) e^{-(E_f + \mu_f)/T} + e^{-3(E_f + \mu_f)/T}]. \end{aligned} \quad (\text{A16b})$$

From this thermodynamic potential the equations of motion for the mean fields σ_u , σ_d , Φ , and $\bar{\Phi}$ are derived through

$$\frac{\partial \Omega}{\partial \sigma_u} = 0, \quad \frac{\partial \Omega}{\partial \sigma_d} = 0, \quad \frac{\partial \Omega}{\partial \Phi} = 0, \quad \frac{\partial \Omega}{\partial \bar{\Phi}} = 0. \quad (\text{A17})$$

These coupled equations are then solved for the fields as functions of T , μ_u , and μ_d . They give

$$\sigma_f = -6 \int \frac{d^3 p}{(2\pi)^3} \frac{m_f}{E_f} [\theta(\Lambda^2 - p^2) - \mathcal{N}(E_f)\mathcal{M}(E_f) - \bar{\mathcal{N}}(E_f)\bar{\mathcal{M}}(E_f)]; \quad f = u, d, \quad (\text{A18a})$$

$$\frac{\partial \mathcal{U}}{\partial \Phi} = 6T \sum_{f=u,d} \int \frac{d^3 p}{(2\pi)^3} [\mathcal{N}(E_f)e^{-(E_f-\mu_f)/T} + \bar{\mathcal{N}}(E_f)e^{-2(E_f+\mu_f)/T}], \quad (\text{A18b})$$

$$\frac{\partial \mathcal{U}}{\partial \bar{\Phi}} = 6T \sum_{f=u,d} \int \frac{d^3 p}{(2\pi)^3} [\mathcal{N}(E_f)e^{-2(E_f-\mu_f)/T} + \bar{\mathcal{N}}(E_f)e^{-(E_f+\mu_f)/T}], \quad (\text{A18c})$$

$$\mathcal{N}(E_f) = [1 + 3(\Phi + \bar{\Phi}e^{-(E_f-\mu_f)/T})e^{-(E_f-\mu_f)/T} + e^{-3(E_f-\mu_f)/T}]^{-1}, \quad (\text{A18d})$$

$$\bar{\mathcal{N}}(E_f) = [1 + 3(\bar{\Phi} + \Phi e^{-(E_f+\mu_f)/T})e^{-(E_f+\mu_f)/T} + e^{-3(E_f+\mu_f)/T}]^{-1}, \quad (\text{A18e})$$

$$\mathcal{M}(E_f) = (\Phi + 2\bar{\Phi}e^{-(E_f-\mu_f)/T})e^{-(E_f-\mu_f)/T} + e^{-3(E_f-\mu_f)/T}, \quad (\text{A18f})$$

$$\bar{\mathcal{M}}(E_f) = (\bar{\Phi} + 2\Phi e^{-(E_f+\mu_f)/T})e^{-(E_f+\mu_f)/T} + e^{-3(E_f+\mu_f)/T}. \quad (\text{A18g})$$

Finally we note that the values of the parameters used are exactly the same as those used in Ref. [29].

-
- [1] L.D. McLerran and B. Svetitsky, Phys. Rev. D **24**, 450 (1981); B. Svetitsky and L.G. Yaffe, Nucl. Phys. **B210**, 423 (1982); B. Svetitsky, Phys. Rep. **132**, 1 (1986).
- [2] R.D. Pisarski, Phys. Rev. D **62**, 111501(R) (2000); R.D. Pisarski in *Proceedings of Marseille 2000, Strong and Electroweak Matter*, edited by C.P. Korthals Altes (World Scientific, Singapore, 2001), pp. 107–117 [hep-ph/0101168].
- [3] E. Megias, E. Ruiz Arriola, and L.L. Salcedo, Phys. Rev. D **69**, 116003 (2004).
- [4] D. Diakonov and M. Oswald, Phys. Rev. D **70**, 105016 (2004).
- [5] A. Dumitru and R.D. Pisarski, Phys. Lett. B **504**, 282 (2001); Phys. Rev. D **66**, 096003 (2002); Nucl. Phys. **A698**, 444 (2002).
- [6] O. Scavenius, A. Dumitru, and J.T. Lenaghan, Phys. Rev. C **66**, 034903 (2002).
- [7] E. Megias, E.R. Arriola, and L.L. Salcedo, J. High Energy Phys. 01 (2006) 073.
- [8] M. Gell-Mann and M. Levy, Nuovo Cimento **16**, 705 (1960).
- [9] Y. Nambu and G. Jona-Lasinio, Phys. Rev. **122**, 345 (1961); **124**, 246 (1961).
- [10] U. Vogl and W. Weise, Prog. Part. Nucl. Phys. **27**, 195 (1991); S.P. Klevansky, Rev. Mod. Phys. **64**, 649 (1992); T. Hatsuda and T. Kunihiro, Phys. Rep. **247**, 221 (1994); M. Buballa, Phys. Rep. **407**, 205 (2005).
- [11] M. Alford, K. Rajagopal, and F. Wilczek, Phys. Lett. B **422**, 247 (1998); R. Rapp, T. Schäfer, E.V. Shuryak, and M. Velkovsky, Phys. Rev. Lett. **81**, 53 (1998).
- [12] J. Berges and K. Rajagopal, Nucl. Phys. **B538**, 215 (1999).
- [13] M.A. Halasz, A.D. Jackson, R.E. Shrock, M.A. Stephanov, and J.J.M. Verbaarschot, Phys. Rev. D **58**, 096007 (1998).
- [14] S.P. Klevansky, Rev. Mod. Phys. **64**, 649 (1992); A. Barducci, R. Casalbuoni, G. Pettini, and R. Gatto, Phys. Rev. D **49**, 426 (1994).
- [15] M.A. Stephanov, Phys. Rev. Lett. **76**, 4472 (1996); Nucl. Phys. B, Proc. Suppl. **53**, 469 (1997).
- [16] M. Stephanov, K. Rajagopal, E. Shuryak, Phys. Rev. Lett. **81**, 4816 (1998).
- [17] H. Abuki and T. Kunihiro, Nucl. Phys. **A768**, 118 (2006).
- [18] Z. Fodor and S.D. Katz, J. High Energy Phys. 04 (2004) 050.
- [19] Z. Fodor and S.D. Katz, J. High Energy Phys. 03 (2002) 014.
- [20] Z. Fodor and S. Katz, Phys. Lett. B **534**, 87 (2002).
- [21] R. V. Gavai and S. Gupta, Phys. Rev. D **71**, 114014 (2005).
- [22] D.T. Son and M.A. Stephanov, Phys. Rev. Lett. **86**, 592 (2001); K. Splittorff, D.T. Son, and M.A. Stephanov, Phys. Rev. D **64**, 016003 (2001); J.B. Kogut and D. Toublan, Phys. Rev. D **64**, 034007 (2001); Y. Nishida, Phys. Rev. D **69**, 094501 (2004); M. Loewe and C. Villavicencio, Phys. Rev. D **71**, 094001 (2005); L. He and P. Zhuang, Phys. Lett. B **615**, 93 (2005); L. He, M. Jin, and P. Zhuang, Phys. Rev. D **71**, 116001 (2005); **74**, 036005 (2006); D. Ebert and K.G. Klimenko, J. Phys. G **32**, 599 (2006); Eur. Phys. J. C **46**, 771 (2006).
- [23] J.B. Kogut and D.K. Sinclair, Phys. Rev. D **66**, 014508 (2002); **66**, 034505 (2002); S. Gupta, arXiv:hep-lat/0202005.
- [24] P.N. Meisinger and M.C. Ogilvie, Phys. Lett. B **379**, 163 (1996); Nucl. Phys. B, Proc. Suppl. **47**, 519 (1996).
- [25] K. Fukushima, Phys. Lett. B **591**, 277 (2004).
- [26] E. Megias, E.R. Arriola, and L.L. Salcedo, Phys. Rev. D **74**, 065005 (2006); **74**, 114014 (2006); S. Digal, arXiv:hep-ph/0605010.
- [27] F. Karsch and E. Laermann, Phys. Rev. D **50**, 6954 (1994).
- [28] C. Ratti, M.A. Thaler, and W. Weise, Phys. Rev. D **73**, 014019 (2006).
- [29] S.K. Ghosh, T.K. Mukherjee, M.G. Mustafa, and R. Ray, Phys. Rev. D **73**, 114007 (2006).
- [30] H. Hansen *et al.*, Phys. Rev. D **75**, 065004 (2007).
- [31] C.R. Allton *et al.*, Phys. Rev. D **71**, 054508 (2005).
- [32] R. V. Gavai and S. Gupta, Phys. Rev. D **73**, 014004 (2006).

- [33] M. Frank, M. Buballa, and M. Oertel, *Phys. Lett. B* **562**, 221 (2003).
- [34] M. Asakawa and K. Yazaki, *Nucl. Phys.* **A504**, 668 (1989).
- [35] D. Toublan and J.B. Kogut, *Phys. Lett. B* **564**, 212 (2003).
- [36] B. Klein, D. Toublan, and J. J. M. Verbaarschot, *Phys. Rev. D* **68**, 014009 (2003).
- [37] A. Barducci, G. Pettini, L. Ravagli, and R. Casalbuoni, *Phys. Lett. B* **564**, 217 (2003).
- [38] D. Toublan and J. B. Kogut, *Phys. Lett. B* **605**, 129 (2005).
- [39] L. He, M. Jin, and P. Zhuang, *Mod. Phys. Lett. A* **22**, 637, (2007).
- [40] H. Reinhardt and R. Alkofer, *Phys. Lett. B* **207**, 482 (1988).
- [41] V. Bernard, R.L. Jaffe, and U.-G. Meissner, *Nucl. Phys.* **B308**, 753 (1988).
- [42] A. Barducci, R. Casalbuoni, G. Pettini, and L. Ravagli, *Phys. Rev. D* **69**, 096004 (2004).
- [43] D. Toublan, arXiv:hep-ph/0511138.
- [44] L. Stodolsky, *Phys. Rev. Lett.* **75**, 1044 (1995).
- [45] R. Korus, S. Mrowczynski, M. Rybczynski, and Z. Włodarczyk, *Phys. Rev. C* **64**, 054908 (2001).
- [46] J. Y. Ollitrault, *Phys. Rev. D* **46**, 229 (1992).
- [47] H. Sorge, *Phys. Rev. Lett.* **82**, 2048 (1999).
- [48] P. F. Kolb *et al.*, *Phys. Lett. B* **459**, 667 (1999); *Nucl. Phys.* **A661**, 349 (1999).
- [49] D. Teaney, J. Lauret, and E. V. Shuryak, *Phys. Rev. Lett.* **86**, 4783 (2001); D. Teaney *et al.*, arXiv:nucl-th/0110037.
- [50] G. Boyd *et al.*, *Nucl. Phys.* **B469**, 419 (1996); Y. Iwasaki, K. Kanaya, T. Kaneko, and T. Yoshie, *Phys. Rev. D* **56**, 151 (1997).
- [51] B. Beinlich *et al.*, *Eur. Phys. J. C* **6**, 133 (1999); M. Okamoto *et al.*, *Phys. Rev. D* **60**, 094510 (1999).
- [52] P. de Forcrand *et al.*, *Nucl. Phys.* **B577**, 263 (2000); Y. Namekawa *et al.*, *Phys. Rev. D* **64**, 074507 (2001).
- [53] P.N. Messinger, M.C. Ogilvie, and T.R. Miller, *Phys. Lett. B* **585**, 149 (2004).
- [54] S. Roszner, C. Ratti, W. Weise, *Phys. Rev. D* **75**, 034007 (2007).
- [55] Z. Zhang and Y-X Liu, arXiv:hep-ph/0610221.
- [56] R. V. Gavai and S. Gupta, *Phys. Rev. D* **72**, 054006 (2005).
- [57] C. Ratti, M. A. Thaler, and W. Weise, arXiv:nucl-th/0604025.
- [58] A. Dumitru, R. D. Pisarski, and D. Zschiesche, *Phys. Rev. D* **72**, 065008 (2005).
- [59] C. Sasaki, B. Friman, and K. Redlich, *Phys. Rev. D* **75**, 054026 (2007).
- [60] C.R. Allton *et al.*, *Phys. Rev. D* **66**, 074507 (2002).
- [61] J.B. Kogut and D.K. Sinclair, *Phys. Rev. D* **70**, 094501 (2004).
- [62] B. Mohanty and Jan-e Alam, *Phys. Rev. C* **68**, 064903 (2003).
- [63] S. Mukherjee, *Phys. Rev. D* **74**, 054508 (2006).
- [64] D. Ebert, K. G. Klimenko, V.Ch. Zhukovsky, and A. M. Fedotov, *Eur. Phys. J. C* **49**, 709 (2007).